

# Mechanical properties and microstructures of $\text{Al}_2\text{O}_3$ –5 vol.% YAG composites

Hongzhi Wang<sup>a</sup>, Lian Gao<sup>a,\*</sup>, Zhijian Shen<sup>b</sup>, Mats Nygren<sup>b,\*1</sup>

<sup>a</sup>*Shanghai Institute of Ceramics, Chinese Academy of Sciences, Shanghai 200050, People's Republic of China*

<sup>b</sup>*Department of Inorganic Chemistry, Arrhenius Laboratory, Stockholm University, S-106 91 Stockholm, Sweden*

Received 30 March 2000; received in revised form 22 August 2000; accepted 31 August 2000

## Abstract

$\text{Al}_2\text{O}_3$ –5 vol.% YAG powder mixtures were prepared by three different methods: (i) Calcination of co-precipitated Al- and Y-hydroxides; (ii) precipitation of  $\text{Al}(\text{OH})_3$  in a slurry containing nano-sized YAG particles, followed by calcination; (iii) ball milling of  $\text{Al}_2\text{O}_3$  and YAG particles. Almost fully dense  $\text{Al}_2\text{O}_3$ –5 vol.% YAG compacts were obtained by hot-pressing these powders at a temperature equal to or exceeding 1550°C. Mechanical tests performed at room temperature showed that the bending strength of the  $\text{Al}_2\text{O}_3$ –5 vol.% YAG composite prepared from powder (i) was 604 MPa, and the fracture toughness 5.0 MPa m<sup>1/2</sup>, whereas compacts of the other two powders had lower bending strength and fracture toughness values. Microstructure investigations revealed a homogeneous distribution of YAG in the  $\text{Al}_2\text{O}_3$  matrix in the compacts prepared from the powders (i) and (ii), although some nano-sized pores were found within the  $\text{Al}_2\text{O}_3$  matrix prepared from powder (i). © 2001 Elsevier Science Ltd. All rights reserved.

**Keywords:**  $\text{Al}_2\text{O}_3$ –YAG; Composites; Mechanical properties; Microstructure-final; YAG

## 1. Introduction

Non-oxide ceramics such as  $\text{SiC}$  and  $\text{Si}_3\text{N}_4$  have attractive mechanical properties at high temperatures, but they are easily oxidized in air at temperatures above approximately 1500°C. Oxide ceramics have excellent oxidation resistance and can more easily be sintered to full density than the non-oxide ceramics, but they have lower creep resistance, which limits their usefulness at high temperature.

Single crystals of yttrium-aluminum-garnet,  $\text{Y}_3\text{Al}_5\text{O}_{12}$  (YAG), exhibit excellent creep resistance and so do polycrystalline compacts, as shown by Parthasarathy and Corman et al., which indicates that YAG ought to be a suitable matrix and/or reinforcing material.<sup>1,2</sup>

Most previous studies on  $\text{Al}_2\text{O}_3$ –YAG composites have been focused on composites with eutectic compositions and on YAG fiber reinforced ceramics,<sup>3–5</sup> but very little is known about YAG particle reinforced alumina

ceramics.<sup>6</sup> Since YAG has a high melting point and similar thermal expansion coefficient as  $\text{Al}_2\text{O}_3$ , it should be of interest to study the mechanical properties of YAG particle reinforced  $\text{Al}_2\text{O}_3$  ceramics.

Pseudo-binary or ternary powder mixtures are frequently prepared by mechanical mixing, but it is often difficult to obtain homogeneously distributed components by this method.  $\text{Al}_2\text{O}_3$ – $\text{SiC}$  composites containing homogeneously distributed nano-sized  $\text{SiC}$  particles have previously been prepared from a precursor powder mixture prepared by a heterogeneous precipitation method similar to the one used in this study.<sup>7</sup> Another method to obtain a homogeneous distribution of Y and Al is to co-precipitate these ions, e.g. from a water solution and then heat treating the precipitate at an appropriate temperature, hopefully making yttria react completely with alumina to form YAG. This method to prepare precursor powder mixtures and sintered compacts of  $\text{Al}_2\text{O}_3$ –YAG is also evaluated in this article. Finally, a precursor powder mixture may be prepared by the standard mechanical mixing procedure. The aimed-at composition in the present work was all cases  $\text{Al}_2\text{O}_3$ –5 vol.% YAG.

\* Corresponding author.

<sup>1</sup> Tel.: +46-8-162366; fax: +46-8-152187.

E-mail address: mats@inorg.su.se (M. Nygren).

Dense compacts of these powder mixtures were obtained by hot pressing, and their phase compositions were evaluated from X-ray powder diffraction patterns. Their mechanical properties — bending strength and fracture toughness — were determined and their microstructures were also evaluated.

## 2. Experimental

$\text{Al}_2\text{O}_3$ –5 vol.% YAG powders were prepared by three different methods: (i) appropriate amounts of  $\text{Al}(\text{NO}_3)_3$  and  $\text{Y}(\text{NO}_3)_3$  were dissolved in distilled water, and ammonia and water were added so as to keep pH between 8 and 9. The obtained precipitate was first washed with distilled water and ethanol, then dried at 100°C and finally calcinated at different temperatures (see below) for 2 h. This method will be named the co-precipitation method; (ii)  $\text{AlCl}_3$  (Shanghai Jinshan Chemical Co., China) was added to an aqueous solution containing 0.2  $\mu\text{m}$ -sized YAG particles (Seattle Special Ceramics, Inc., USA), and water was added as above, keeping pH between 9 and 10. The  $\text{Al}(\text{OH})_3$ –YAG precipitate was dried at 100°C and calcinated at 700°C which, according to X-ray and scanning electron microscope (SEM) studies, yielded a homogeneously mixed  $\text{Al}_2\text{O}_3$ –YAG powder; (iii)  $\text{Al}_2\text{O}_3$  powder with an average particle size of 0.3  $\mu\text{m}$  (Shanghai WuSong Chemical Co., China) and YAG powder (as above) were ball milled together in ethanol for 12 h, using zirconia balls as milling media. The obtained mixture was dried and de-agglomerated.

These powders were hot pressed between 1400 and 1650°C in  $\text{N}_2$  atmosphere for 1 h, at a pressure of 30 MPa.

The X-ray diffraction (XRD) patterns of the powders and sintered compacts were recorded in an X-ray powder diffraction unit (Rigaku D/max-*ra*) with  $\text{CuK}_{\alpha_1}$  radiation and using Si as internal standard.

To obtain information about the formation of YAG by the co-precipitation method, calcinated powders and pre-pressed bodies were heat treated at different temperatures, and the phases formed were determined from XRD patterns. The densities of the compacted samples were determined according to Archimedes' principle. The hot-pressed samples were cut and polished into rectangular bar specimens ( $4 \times 3 \times 30 \text{ mm}^3$ ). Their fracture strength was determined by the three-point bending method, and fracture toughness was determined by Vickers's indentation method.

The microstructures of sintered compacts were studied in an SEM (EPMA-8705QHII) equipped with an energy-dispersive spectrometer (EDS, Link ISIS), an Auger SEM (Micro-Lab 310F) equipped with an Auger electron spectrometer and in a transmission electron microscope (TEM, JEOL-200CX). The EDS and AES were used for elemental analysis.

## 3. Result and discussion

### 3.1. Powder preparation

The  $\text{Y}_2\text{O}_3$ – $\text{Al}_2\text{O}_3$  system phase diagram<sup>8</sup> reveals that  $\text{Al}_2\text{O}_3$  and YAG can coexist up to 1800°C in the  $\text{Al}_2\text{O}_3$ -rich field. This observation is used when preparing precursor powders according to the co-precipitation method described above. The X-ray diffraction pattern of the obtained dried precipitate revealed the presence of bayerite [ $\alpha$ - $\text{Al}(\text{OH})_3$ ], and the pattern contained some very broad peaks indicating that amorphous yttrium hydroxide had also been formed. When the calcination temperature was increased to above 400°C, the reflections of bayerite disappeared and weak reflections that could be ascribed  $\gamma$ - $\text{Al}_2\text{O}_3$  appeared, which persisted up to a calcination temperature of 1000°C. The XRD patterns of samples calcinated at 1200°C contained reflections that could be ascribed to YAG,  $\alpha$ - $\text{Al}_2\text{O}_3$  and  $\text{YAlO}_3$ . Finally, calcinations at 1300°C yielded a powder mixture of stoichiometric YAG and  $\alpha$ - $\text{Al}_2\text{O}_3$ .

The zeta potential of an aqueous solution containing YAG particles is plotted versus the pH of the solution in Fig. 1. It shows that the isoelectric point of this YAG slurry is located at pH = 8. Thus, in a YAG slurry with pH ≈ 10 the YAG particles will repel each other, and agglomeration is avoided. A slurry of YAG particles with pH ≈ 10 was ultrasonically vibrated for 1 h, and then an aqueous solution of  $\text{AlCl}_3$  and ammonia was added dropwise. When an appropriate amount of  $\text{AlCl}_3$  had been added, the solution was dried and calcinated in air at 700°C for 1 h. The XRD pattern of this powder showed the presence of  $\gamma$ - $\text{Al}_2\text{O}_3$  and YAG.

### 3.2. Sintering

The precursor powders (i), (ii), and (iii) were hot pressed in  $\text{N}_2$  atmosphere at different temperatures for 1 h, using a pressure of 30 MPa. The obtained densities of

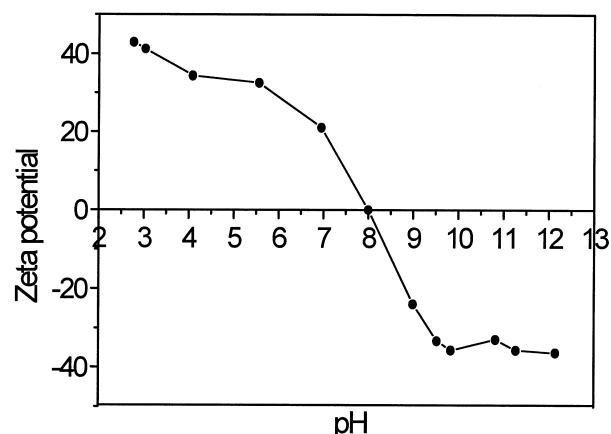


Fig. 1. The zeta potential of YAG particles plotted versus the pH value of the solution.

the sintered compacts are plotted versus the sintering temperature in Fig. 2. Relative densities of 99% or higher were obtained with the precursor powders (i) and (ii) at sintering temperatures equal to or exceeding 1500°C, whereas corresponding temperatures for the ball mixed powder were 1550°C, i.e. in the same temperature range as monolithic Al<sub>2</sub>O<sub>3</sub> is prepared. The precursor powder obtained from the co-precipitation method was calcined at 700°C prior to hot-pressing. As shown above, this powder undergoes a series of phase transformations upon heat treatment to temperatures exceeding 1300°C. The obtained compacts did not exhibit any cracks, and the XRD patterns of these compacts showed no other phases than YAG and Al<sub>2</sub>O<sub>3</sub> (see Fig. 3).

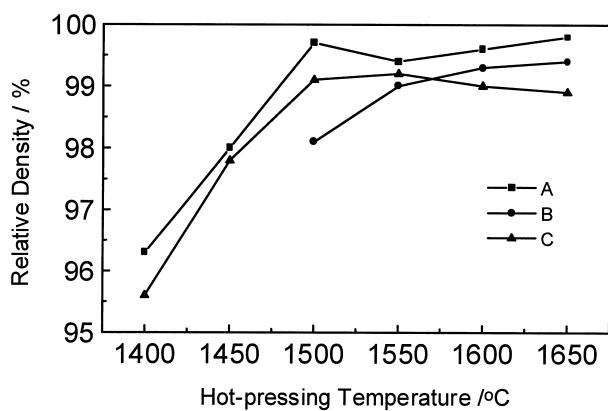


Fig. 2. Relative density of sintered bodies plotted versus the hot-pressing temperature: A, powder (ii); B, powder (iii); C, powder (i).

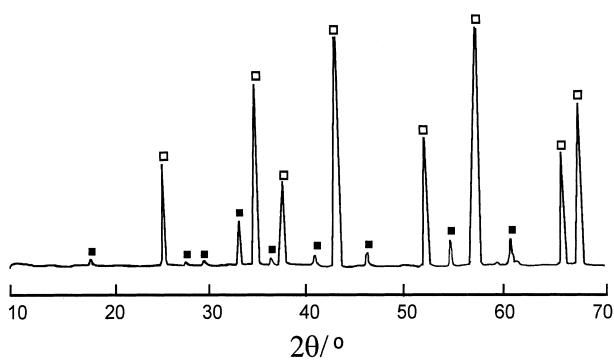


Fig. 3. XRD diffractrogram of an Al<sub>2</sub>O<sub>3</sub>-5 vol.% YAG composite prepared from powder (i) and hot-pressed at 1550°C (■ and □ represent YAG and α-Al<sub>2</sub>O<sub>3</sub>, respectively).

### 3.3. Mechanical properties

The mechanical properties of compacted samples obtained at 1500 and 1650°C are compiled in Table 1. The bending strength and fracture toughness values of the compacts prepared from the precursor powder (i) are substantially higher than those obtained for the powders (ii) and (iii). The values are higher than typical data obtained for monolithic Al<sub>2</sub>O<sub>3</sub> prepared under similar conditions, namely 350 MPa and 3.2 MPa m<sup>1/2</sup> for the bending strength and fracture toughness, respectively.<sup>9</sup> This indicates that the mechanical properties of Al<sub>2</sub>O<sub>3</sub> ceramics are improved by the incorporation of YAG. We have not been able to explain the large spread in the bending strength measurements of sample (iii). With increasing sintering temperature the mechanical properties deteriorate. SEM micrographs depicting the fracture surfaces of samples prepared at 1650°C are given in Fig. 4. The grains are coarser in the sample prepared from ball-mixed powder than in the others, and we tentatively ascribe the lower bending strength of this sample to that observation.

### 3.4. Microstructure

A TEM micrograph of the Al<sub>2</sub>O<sub>3</sub>-5 vol.% YAG composite prepared from powder (ii) is given in Fig. 5. The YAG particles are uniformly distributed in the Al<sub>2</sub>O<sub>3</sub> matrix; most of them are, however, located within the Al<sub>2</sub>O<sub>3</sub> grains rather than at the grain boundaries. A TEM micrograph of a composite prepared from precursor

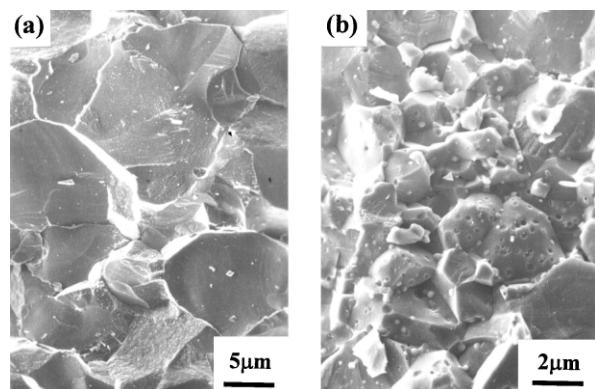


Fig. 4. SEM micrographs of the fractured surface of samples prepared from (a) powder (iii) and powder (ii), by hot pressing at 1650°C.

Table 1  
Summary of obtained mechanical properties of Al<sub>2</sub>O<sub>3</sub>-5vol.% YAG composites

Sintering Temp. (°C)	1500			1650		
Precursor powder <sup>a</sup>	(i)	(ii)	(iii)	(i)	(ii)	(iii)
Bending strength (MPa)	604±25	485±28	432±140	402±21	284±4	111±14
Fracture toughness (MPa m <sup>1/2</sup> )	5.0±0.5	4.2±0.5	4.2±0.6	4.1±0.1	4.0±0.1	3.5±0.4

<sup>a</sup> Precursor powders prepared according to the (i) co-precipitation, (ii) heterogeneous precipitation, and (iii) ball mixing methods, respectively; see text.

powder (i) is given in Fig. 6a, and it shows that the grain size of  $\text{Al}_2\text{O}_3$  matrix is of the order 2–4  $\mu\text{m}$ , that some large YAG particles (about 1  $\mu\text{m}$ ) are located at the grain boundaries of  $\text{Al}_2\text{O}_3$  and some small YAG particles (100–200 nm) within the  $\text{Al}_2\text{O}_3$  grains. In addition, quite a few small white areas are seen inside  $\text{Al}_2\text{O}_3$

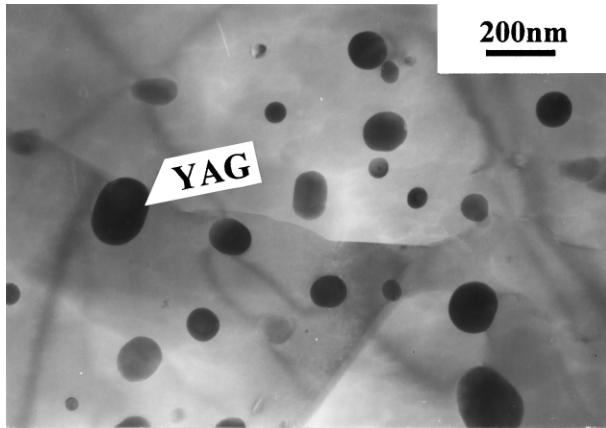


Fig. 5. TEM micrograph of  $\text{Al}_2\text{O}_3$ -5 vol.% YAG composite prepared from powder (ii).

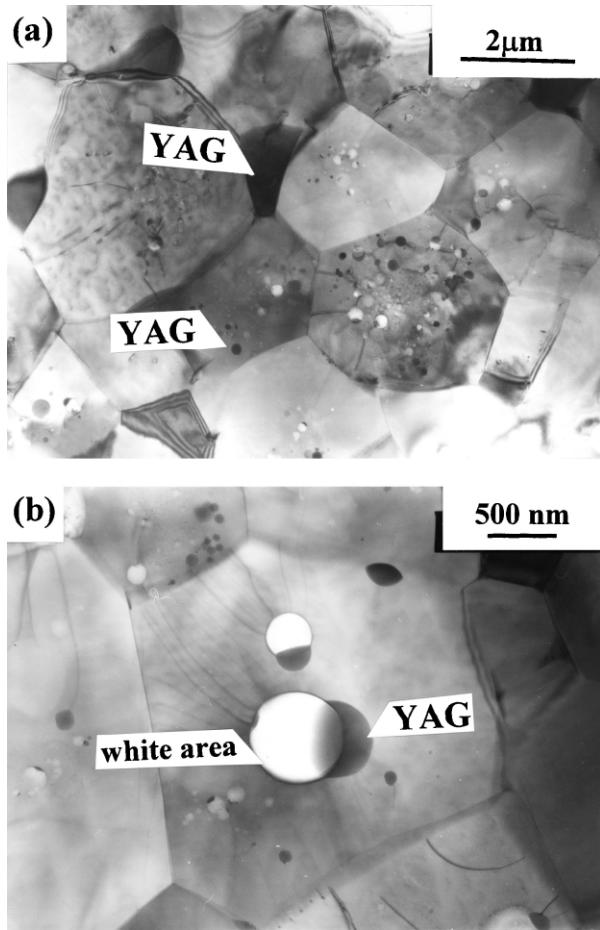


Fig. 6. TEM micrograph of the  $\text{Al}_2\text{O}_3$ -5 vol.% YAG composite prepared from powder (i).

grains. These areas are usually close to or partly overlap the YAG particles also present within the  $\text{Al}_2\text{O}_3$  grain, as seen in Fig. 6b. SEM-EDS elemental analysis of a thin flake revealed that no elements other than Al and O were present within these white areas. An Auger SEM

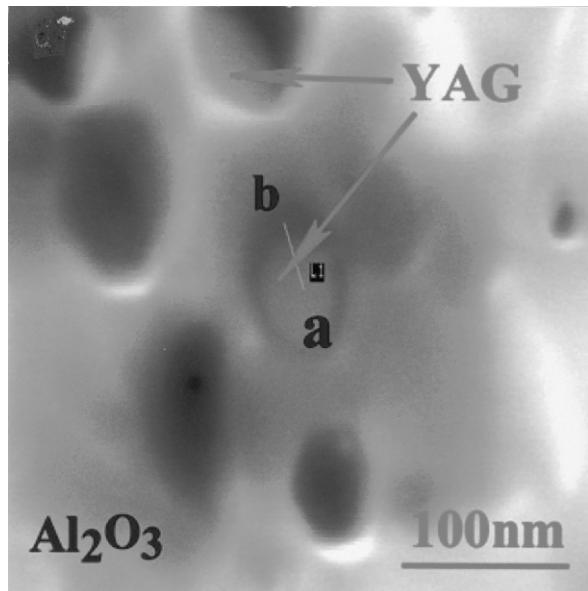


Fig. 7. Auger SEM micrograph of the  $\text{Al}_2\text{O}_3$ -5 vol.% YAG composite prepared from powder (i).

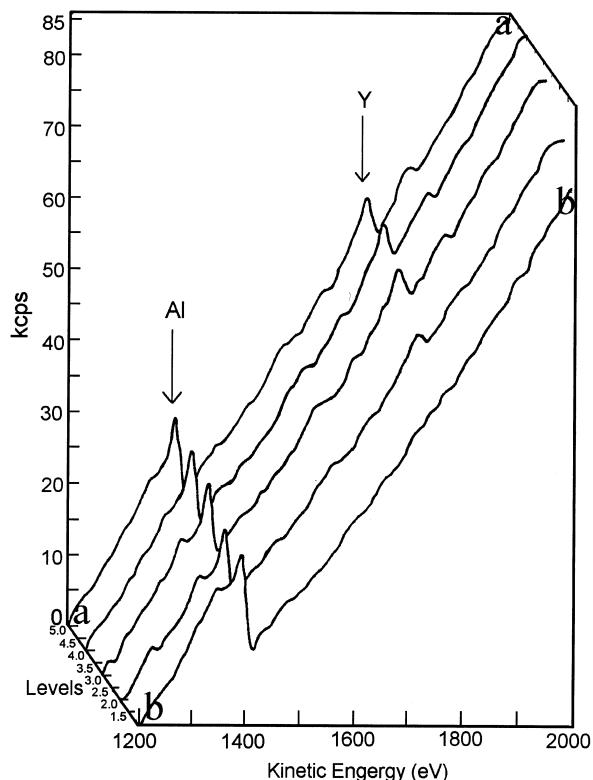


Fig. 8. Auger electron spectrogram of the composite  $\text{Al}_2\text{O}_3$ -5 vol.% YAG prepared from powder (i) and recorded between the points a and b marked in Fig. 7.

micrograph of a similar thin flake containing one white area is shown in Fig. 7. The Auger electron spectrogram between the points a and b marked in Fig. 7 is given in Fig. 8. This figure reveals that the Y content is lower inside the white area than outside, in accordance with the observation that a lower Y content gives rise to lighter contrast in a TEM micrograph. The most probable explanation is that these white areas represent nano-sized pores. Probably, some  $\text{Y}_2\text{O}_3$  and/or  $\text{Y}(\text{OH})_3$  nano-sized grains have initially been encapsulated by the  $\text{Al}_2\text{O}_3$  matrix and have later reacted with the matrix to form YAG, leaving a pore behind. This interpretation is also supported by the fact that such white areas were never observed in samples prepared from the powders (ii) and (iii). The occurrence of these nano-sized pores within the  $\text{Al}_2\text{O}_3$  matrix seems, however, not to degrade the mechanical properties of the composite.

#### 4. Conclusions

Three different precursor powder mixtures of the composition  $\text{Al}_2\text{O}_3$ –5 vol.% YAG have been prepared and compacted to a relative density of 99% or better by hot pressing. The bending strength and fracture toughness of the compacts sintered at 1500°C were found to be higher than corresponding data obtained for monolithic  $\text{Al}_2\text{O}_3$  prepared under similar conditions. The precursor powder (i), prepared by the co-precipitation method, yielded compacts with the best bending strength and fracture toughness values,  $604 \pm 25$  MPa and  $5.0 \pm 0.5$  MPa  $\text{m}^{1/2}$ .

Microstructure studies revealed that most of the YAG particles were located within the  $\text{Al}_2\text{O}_3$  grains in compacts prepared from powder mixtures (i) and (ii) and that compacts prepared from mixture (i) contained nano-sized pores within the  $\text{Al}_2\text{O}_3$  grains. It is suggested that these areas are formed when initially encapsulated  $\text{Y}_2\text{O}_3$  and/or  $\text{Y}(\text{OH})_3$  nano-sized grains react with the  $\text{Al}_2\text{O}_3$  matrix to form YAG.

#### References

1. Mah, T., Parthasarathy, T. and Matson, L., Processing and mechanical properties of  $\text{Al}_2\text{O}_3/\text{Y}_3\text{Al}_5\text{O}_{12}$ (YAG) eutectic composite. *Ceram. Eng. Sci. Proc.*, 1990, **11**, 1617–1627.
2. Keller, K., Mah, T. and Parthasarathy, A., Processing and mechanical properties of polycrystalline  $\text{Y}_3\text{Al}_5\text{O}_{12}$ . *Ceram. Eng. Sci. Proc.*, 1990, **11**, 1122–1133.
3. Matson, L., Hay, R. and Mah, T., Characterization of alumina/yttrium-aluminum garnet and alumina/yttrium-aluminum perovskite eutectics. *Ceram. Eng. Sci. Proc.*, 1990, **11**, 995–1003.
4. Duong, H. and Wolfenstine, J., Creep-behavior of fine-grained two-phase  $\text{Al}_2\text{O}_3$ – $\text{Y}_3\text{Al}_5\text{O}_{12}$  materials. *Mater. Sci. Eng.*, 1993, **A172**, 173–179.
5. Hay, R., Fiber-matrix interfaces for alumina fiber–YAG matrix composites. *Ceram. Eng. Sci. Proc.*, 1990, **11**, 1526–1535.
6. Shen, Z., Ekstrand, Å and Nygren, M., Oxide/oxide composites in the system  $\text{Cr}_2\text{O}_3$ – $\text{Y}_2\text{O}_3$ – $\text{Al}_2\text{O}_3$ . *J. Eur. Ceram. Soc.*, 2000, **20**, 625–630.
7. Wang, H. Z., Gao, L., Gui, L. H. and Guo, J. K., Preparation and properties of intergranular  $\text{Al}_2\text{O}_3$ –SiC nanocomposites. *NanoStructured Materials*, 1998, **10**, 947–953.
8. Levin, E., Robbins, C., McMurdie, H. M., (Ed.), *Phase Diagrams for Ceramists 1969 Supplement*. The Am. Ceram. Soc. Pub., Columbus, OH, 1969, p. 96, Figs. 2344–2347.
9. Niihara, K., New design concept of structural ceramics — ceramic nanocomposites, *J. Ceram. Soc. Jpn.*, 1991, 974–982.